Fusion Engineering and Design 109–111 (2016) 586–589

Contents lists available at ScienceDirect

Fusion Engineering and Design

journal homepage: www.elsevier.com/locate/fusengdes

Surface condition effects on tritium permeation through the first wall of a water-cooled ceramic breeder blanket

H.-S. Zhou[a], Y.-P. Xu[b], H.-D. Liu[b], F. Liu[a], X.-C. Li[a], M.-Z. Zhao[a], Q. Qi[a], F. Ding[a], G.-N. Luo[a,b,c,d,*]

[a] Institute of Plasma Physics, Chinese Academy of Sciences, P.O. Box 1126, Hefei, China
[b] Science Island Branch of Graduate School, University of Science and Technology of China, P.O. Box 1126, Hefei, China
[c] Hefei Center for Physical Science and Technology, P.O. Box 1126, Hefei, China
[d] Hefei Science Center of Chinese Academy of Science, P.O. Box 1126, Hefei, China

HIGHLIGHTS

- We investigate surface effects on T transport through the first wall.
- We solve transport equations with various surface conditions.
- The RAFMs walls w/and w/o W exhibit different T permeation behavior.
- Diffusion in W has been found to be the rate-limiting step.

ARTICLE INFO

Article history:
Received 17 September 2015
Received in revised form 28 January 2016
Accepted 13 February 2016
Available online 28 February 2016

Keywords:
Tritium
First wall
Permeation
WCCB blanket
RAFMs
Tungsten

ABSTRACT

Plasma-driven permeation of tritium (T) through the first wall of a water-cooled ceramic breeder (WCCB) blanket may raise safety and other issues. In the present work, surface effects on T transport through the first wall of a WCCB blanket have been investigated by theoretical calculation. Two types of wall structures, i.e., reduced activation ferritic/martensitic steels (RAFMs) walls with and without tungsten (W) armor, have been analyzed. Surface recombination is assumed to be the boundary condition for both the plasma-facing side and the coolant side. It has been found that surface conditions at both sides can affect T permeation flux and inventory. For the first wall using W as armor material, T permeation is not sensitive to the plasma-facing surface conditions. Contamination of the surfaces will lead to higher T inventory inside the first wall.

1. Background

Deuterium (D) and tritium (T) will migrate through the first wall of magnetic fusion reactors by a phenomenon called plasma-driven permeation (PDP) [1–4]. For the water-cooled ceramic breeder (WCCB) blanket [5], which is a candidate concept for the China Fusion Engineering Test Reactor (CFETR) [6], T PDP into the coolant will produce massive radioactive water. This total T permeation amount must be carefully evaluated because it is one of the key input parameters for nuclear safety analysis and T recovery system design.

Hydrogen isotope PDP through the first wall is controlled by two possible rate-limiting steps, i.e., diffusion in the bulk and recombination at the surface [7]. Diffusivity is one of the intrinsic material properties, while the recombination process is determined by the surface condition. Under reactor operational conditions, the plasma-facing side of the first wall would not be smooth and clean. The wall will be either covered by contaminations or eroded by plasma bombardment, making it even more difficult to predict the T permeation flux [8,9].

In our recent studies on WCCB blanket [5], reduced activation ferritic/martensitic steels (RAFMs) are selected as the structure material and an additional tungsten (W) layer on the plasma-facing side is considered as an armor and as well as tritium permeation barrier. Due to the notable differences in hydrogen transport parameters of RAFMs and W, the T permeation behavior through

* Corresponding author at: P.O. 1126, Hefei, Anhui 230031, China.
E-mail address: gnluo@ipp.ac.cn (G.-N. Luo).

http://dx.doi.org/10.1016/j.fusengdes.2016.02.041
0920-3796/

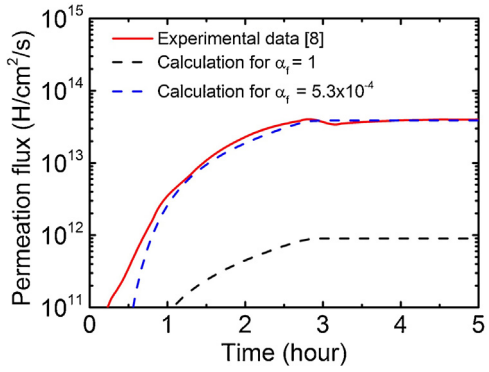

Fig. 1. Evaluation of surface sticking property of H on F82H from a PDP experiment [8] at a temperature around 800 K.

a multi-layer W + RAFMs wall may significantly differ from that through a bare RAFMs wall. Nakamura et al. [10] evaluated the T inventory for such a specific wall. His analysis is based on clean surface assumption. Another group, Ogorodnikova et al. [11] made a systematic analysis for surface condition effects on T permeation through the first wall of the EU-HCPB blanket. Different front and back wall conditions were considered, but their data are dedicated to bare RAFMs walls, which cannot be directly used for our WCCB design activities.

In the present work, surface effects on T transport through the first wall of the WCCB blanket have been studied by solving hydrogen transport equations with various surface boundary conditions. Significant differences in T permeation and retention behavior have been found between the first walls with and without W armor material. Rate-limiting steps for those surface conditions are also discussed.

2. Theory and calculation method

For D–T fusion reactor studies, isotope effects must be taken into account because both D and T are the fuels. Isotope effects on hydrogen transport can be divided into two classes [12], i.e., intrinsic effects and synergistic effects. The former class is related to the differences in the transport properties of each of the individual isotopes, e.g., the isotope dependence of the diffusivity. The latter class is due to the competition of isotopes for traps and the coupling of isotopes through the process of surface recombination.

2.1. Hydrogen transport equations

Taking into account the isotope effects, the one-dimensional hydrogen transport process can be expressed as [13]:

$$\frac{\partial C^j(x,t)}{\partial t} = D_j(T)\frac{\partial^2 C^j(x,t)}{\partial x^2} - \sum_i \frac{\partial C_t^{ij}(x,t)}{\partial t} + G_j(x,t) \quad (1)$$

where $C^j(x,t)$ and $C_t^{ij}(x,t)$ are the concentrations of mobile jth species and trapped jth species in the ith trapping site; D_j is the diffusion coefficient of the jth species; T is the temperature; $G_j(x,t)$ is the hydrogen implantation profile of the jth species. Note that $\sum_i \partial C_t^{ij}(x,t)/\partial t$ equates 0 at steady state, which means the steady state flux is not affected by trapping. Eq. (1) can be solved using hydrogen transport codes such as TMAP [14] and DIFFUSE [13], the latter of which is used in this work.

2.2. Diffusion and surface recombination

From the classical theory, the ratio of hydrogen isotopes diffusivities at a certain temperature is commonly inferred to be equivalent to the inverse ratio of the square root of the masses of the isotopes: $D_T/D_H = \sqrt{m_H/m_T}$ and $D_D/D_H = \sqrt{m_H/m_D}$, where D is the diffusivity and m is the mass of the respective isotope. Experimental data indicate that the inverse square root dependence on mass generally provides a reasonable approximation at elevated temperatures [15,16].

Several expressions for surface recombination coefficient have been proposed by separate researchers, e.g., Pick [17] and Baskes [18]. For these models, surface contamination effects are conveyed by hydrogen sticking coefficient. Baskes' model is expressed as follows:

$$K_{jj'}(T) = \frac{4\alpha c_1}{\rho S_0^2\sqrt{(M_j + M_{j'})T}}\exp(-U_k/kT) \quad (2)$$

where c_1 is the kinetic theory constant [13]; α is the sticking coefficient; ρ is the matrix density, S_0 is the pre-factor of solubility; M is the mass of hydrogenic atoms; U_k is the activation energy for recombination. The sticking constant can vary from 1 (for clean surfaces) to <10^{-6} (for contaminated surfaces) [19,20].

Prior to discussing the WCCB case, we can firstly make a comparison between existing experimental data and theoretical calculations with two surface sticking constants, from which one can clearly see the significance of surface condition effects on PDP (Fig. 1). For the PDP experiment performed in a laboratory facility [8], the sample is 5 mm thickness F82H and a bias of −100 V is applied. The electron temperature and density are measured by a Langmuir probe to be ~3.5 eV and ~3×10^{10} cm^{-3}, respectively. The PDP flux curve has been reproduced by DIFFUSE code using the experimental condition as input parameters. Assuming the surface is clean ($\alpha = 1$), the H PDP flux predicted by DIFFUSE is found to be about one order of magnitude lower than the experimental measurement. Only when a much smaller sticking coefficient value is used, the theoretical prediction can agree with the experiment quite well.

3. Data and conditions used in the calculations

3.1. Hydrogen isotopes transport parameters

Hydrogen isotopes transport parameters used in our calculations are shown in Table 1. The measured diffusion coefficient and Sieverts' constant of F82H are used for RAFMs [21]. Frauenfelder's parameters are selected as the input data for W because his data are taken at relatively high temperatures, in which case tapping effects are insignificant [22]. Then the surface recombination coefficients can be calculated from Eq. (2) by assuming various surface conditions.

Table 1
Diffusion coefficient and Sieverts' constant used in the calculations.

	RAFMs [21]	Tungsten [22]
Diffusion coefficient [cm^2/s]	$D = 7.5 \times 10^{-4}\exp(\frac{-0.14}{kT})$	$D = 4.1 \times 10^{-3}\exp(\frac{-0.39}{kT})$
Sieverts' constant [mol/cm^3/Pa$^{1/2}$]	$S = 3.1 \times 10^{-7}\exp(\frac{-0.25}{kT})$	$S = 1.5 \times 10^{-6}\exp(\frac{-1.0}{kT})$

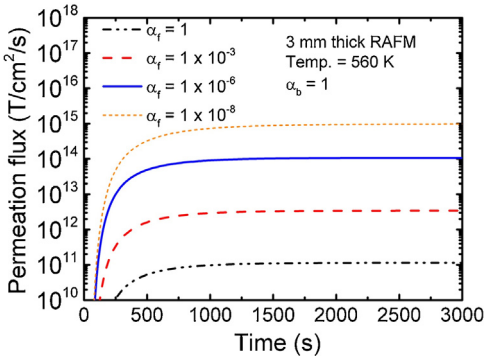

Fig. 2. Effects of the front surface conditions on T PDP flux through a bare RAFMs first wall. The steady state permeation flux has been found to be inversely proportional to the square root of the sticking coefficient.

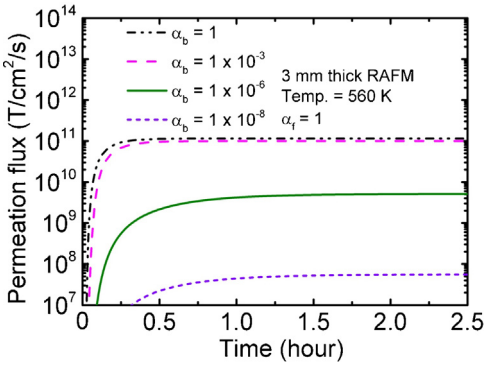

Fig. 3. Effects of the back surface conditions on the T PDP flux through a bare RAFMs first wall.

3.2. First wall conditions assumed for the WCCB blanket

In the conceptual design of the WCCB blanket for CFETR, the first wall is designed to be 3 mm thick made by RAFMs [5]. Then two cases are analyzed in the present work so that we can make a direct comparison between the walls w/and w/o W armor: the first one is a bare 3 mm thick RAFMs wall and the other one is a 3 mm thick RAFMs wall with 2 mm thick W armor. The implanted hydrogenic fluxes (D/T) at the plasma-facing side are assumed to be 1×10^{16} atoms/cm^2/s (5×10^{15} D/cm^2/s and 5×10^{15} T/cm^2/s) with a bombarding energy of 100 eV. The first wall temperature is assumed to be the average value of the inlet (538 K) and outlet (583 K) coolant temperatures. Recombination-limited release is assumed as the boundary condition for both front and back surfaces.

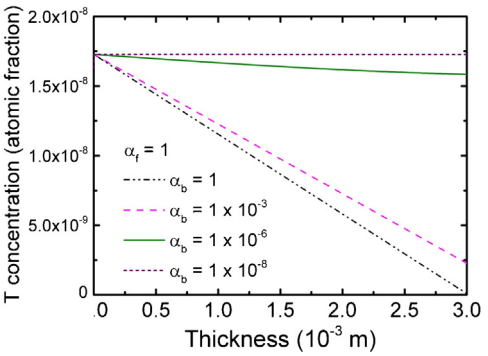

Fig. 4. Effects of the back surface conditions on the steady state T concentration profiles in a bare RAFMs first wall. The front surface (plasma side) is at thickness = 0 mm and the back surface (coolant side) is at thickness = 3 mm.

4. Results and discussion

4.1. Surface condition effects on T PDP through a bare RAFMs wall

Fig. 2 shows the effects of the front surface conditions on T PDP through a bare RAFMs first wall. The front surface sticking coefficient $\alpha_f = 1$ represents a clean surface, while $\alpha_f = 1 \times 10^{-8}$ means the surface is severely contaminated. For a clean back surface (the back surface sticking coefficient $\alpha_b = 1$), the steady state T permeation flux is inversely proportional to the square root of the sticking coefficient α_f at the front surface, which agrees with the theoretical prediction for H PDP taking place in the recombination-diffusion limited regime [16]:

$$J_p = \frac{D}{L}\sqrt{\frac{J_i}{K}} \propto \frac{1}{\sqrt{\alpha_f}} \quad (3)$$

where J_i is the implantation flux and J_p is the permeation flux. L is the membrane thickness.

Assuming the front surface is clean ($\alpha_f = 1$), effects of the back surface conditions on T PDP are also investigated, as shown in Fig. 3 and Fig. 4. Fig. 3 shows the T permeation flux as a function of the back surface sticking coefficient. The results suggest that the permeation flux will decrease if the back surface is contaminated. This behavior can be explained by the steady state T concentration profile shown in Fig. 4. The building-up of T near the back surface leads to a milder T concentration gradient throughout the wall, and as a result, the diffusion-limited permeation flux decreases. This phenomenon is similar to adding a permeation barrier at the coolant side. However, it should be noted that the deceasing in T permeation flux is at the expense of increasing T inventory inside the wall in this case.

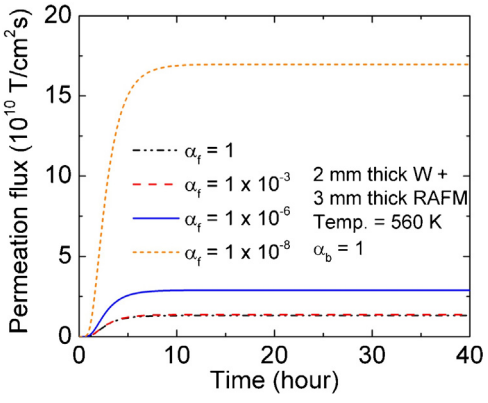

Fig. 5. Effects of the front surface conditions on the T PDP flux through a W + RAFMs first wall.

4.2. Surface condition effects on T PDP through a W + RAFMs first wall

Theoretical and experimental analysis suggests that the total T permeation amount through a bare RAFMs wall of fusion reactors can be as large as tens of grams per day [11,21]. Tungsten, which has relatively low diffusivity and solubility, is a fairly good T barrier material. Surface condition effects on T PDP through a W + RAFMs multi-layer first wall have been investigated as well. Fig. 5 shows the T permeation flux for various front surface sticking coefficients. It can be seen that although the steady state T PDP flux is still affected by the front surface condition, the effects are less sensitive than those on bare RAFMs walls. Further examination of the steady state T concentration profiles (Fig. 6) indicates that the

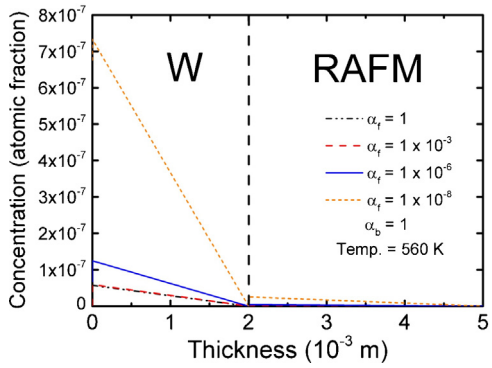

Fig. 6. Effects of the front surface conditions on the steady state T concentration profile in a W + RAFMs first wall. The front surface (plasma side) is at thickness = 0 mm, and the back surface (coolant side) is at thickness = 5 mm.

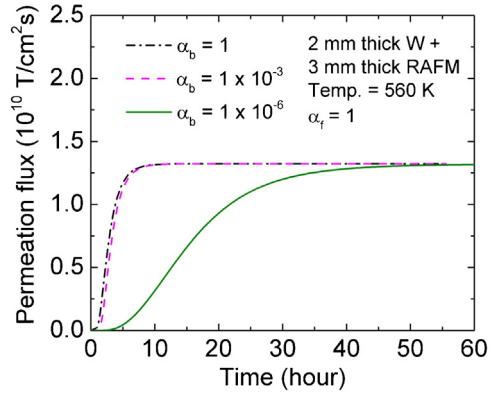

Fig. 7. Effects of the back surface conditions on the T PDP flux through a W + RAFMs first wall. The $\alpha_b = 1 \times 10^{-8}$ case is not shown here because it takes too long to reach steady state.

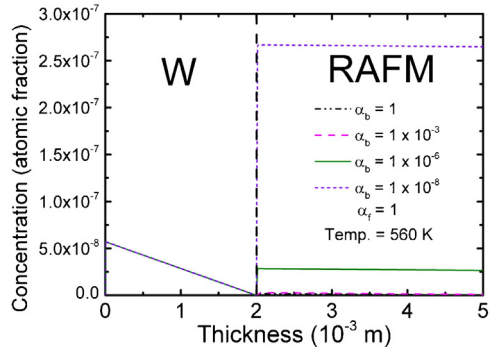

Fig. 8. Effects of the back surface conditions on the steady state T concentration profiles in a W + RAFMs first wall. The front surface (plasma side) is at thickness = 0 mm, and the back surface (coolant side) is at thickness = 5 mm.

permeation process is mainly limited by diffusion in W, which should be due to the low hydrogen isotope diffusivity in W.

This diffusion-limited process can also explain the behavior observed when changing back surface sticking coefficients, as presented in Fig. 7 and Fig. 8. The permeation flux data in Fig. 7 suggest that the steady state T PDP flux is insensitive to the back surface conditions, but the transient T permeation behavior will be slowed down due to the contamination of back surface. Tritium concentration profile in tungsten is not affected by the back surface conditions because of its low T diffusivity and solubility. However, back surface contamination will lead to the build-up of T inventory in RAFMs, which is similar to the bare RAFMs wall case.

5. Conclusions

For the WCCB blankets of CFETR, surface conditions of the first wall will significantly affect the hydrogen isotopes permeation flux and inventory. Contamination of the surfaces will lead to higher T dynamic inventory inside the first wall. Considering that RAFMs are relatively easy to be oxidized, the surface effects warrant further theoretical and experimental investigation to make a more precise prediction on the T permeation amount.

Acknowledgements

The authors would like to thank Prof. Yoshi Hirooka at National Institute for Fusion Science (NIFS), Japan for the discussion on surface sticking property.

This work is supported by National Magnetic Confinement Fusion Science Program of China (Nos. 2013GB105001, 2015GB109001), the National Natural Science Foundation of China (Nos. 11405201), Technological Development Grant of Hefei Science Center of CAS (No. 2014TDG-HSC003), the Korea Research Council of Fundamental Science and Technology (KRCF) under the international collaboration & research in Asian countries (No. PG1314), the Joint Sino-German research project GZ 763.

References

[1] R.A. Causey, et al., The effect of surface composition on plasma driven permeation of deuterium through 304 stainless steel, J. Nucl. Mater. 122–123 (1984) 1547.
[2] Y. Hatano, et al., Influence of surface impurities on plasma-driven permeation of deuterium through nickel, J. Vac. Sci. Technol. A 16 (1998), 2078H.
[3] H. Zhou, et al., Hydrogen plasma-driven permeation through a reduced activation ferritic steel alloy F82H, Fusion Sci. Technol. (2013) 361, T63.
[4] O.V. Ogorodnikova, Surface effects on plasma-driven tritium permeation through metals, J. Nucl. Mater. 290–293 (2001) 459.
[5] S. Liu, et al., Conceptual design of a water cooled breeder blanket for CFETR, Fusion Eng. Des. 89 (2014) 1380.
[6] Y. Song, et al., Concept design of CFETR tokamak machine, IEEE Trans. Plasma Sci. 42 (2014) 503.
[7] B.L. Doyle, A simple theory for maximum H inventory and release: a new transport parameter, J. Nucl. Mater. 111–112 (1982) 628.
[8] Y. Hirooka, et al., Plasma- and gas-driven hydrogen isotope permeation through the first wall of a magnetic fusion power reactor, Fusion Sci. Technol. 64 (2013) 345.
[9] H. Zhou, et al., Effects of surface conditions on the plasma-driven permeation behavior through a ferritic steel alloy observed in VEHICLE-1 and QUEST, J. Nucl. Mater. 463 (2015) 1066.
[10] H. Nakamura, et al., Case study on tritium inventory in the fusion DEMO plant at JAERI, Fusion Eng. Des. 81 (2006) 1339.
[11] O.V. Ogorodnikova, et al., Tritium permeation through the first wall of the EU-HCPB blanket, Fusion Eng. Des. 49–50 (2000) 921.
[12] D.K. Brice, Steady state hydrogen transport in solids exposed to fusion reactor plasmas, part III: isotope effects, J. Nucl. Mater. 122–123 (1984) 1531.
[13] M.I. Baskes, DIFFUSE83, Sandia Report SAND83–8231.
[14] G.R. Longhurst, TMAP7: tritium migration analysis program, user manual, Idaho National Laboratory, INEEL/EXT-04-02352, 2004.
[15] R. Causey, et al., Tritium barriers and tritium diffusion in fusion reactors, in: Comprehensive Nuclear Materials, 1st edition, Elsevier, 2012.
[16] H.H. Johnson, Hydrogen in iron, Met. Trans. A 9 (1988), 2371.
[17] M.A. Pick, et al., A model for atomic hydrogen-metal interactions—application to recycling, recombination and permeation, J. Nucl. Mater. 131 (1985) 208.
[18] M.I. Baskes, A calculation of the surface recombination rate constant for hydrogen isotopes on metals, J. Nucl. Mater. 92 (1980) 318.
[19] O.V. Ogorodnikova, Comparison of hydrogen gas-, atom- and ion-metal interactions, J. Nucl. Mater. 277 (2000) 130.
[20] A.I. Livshitz, Superpermeability of solid membranes and gas evacuation, Vaccum 29 (1979) 103.
[21] H. Zhou, et al., Gas- and plasma-driven hydrogen permeation through a reduced activation ferritic steel alloy F82H, J. Nucl. Mater. 455 (2014) 470.
[22] R. Frauenfelder, Solution and diffusion of hydrogen in tungsten, J. Vac. Sci. Technol. 6 (1969) 388.